High Delta V Nanosatellite Missions using a Diverging Cusped Field Thruster

IEPC-2009-047

Presented at the 31st International Electric Propulsion Conference,
University of Michigan, Ann Arbor, Michigan, USA
September 20–24, 2009

Ryan M. Daspit,* Christopher J. Han,† Paulo Lozano,‡ and David Miller§
Massachusetts Institute of Technology, Cambridge, Massachusetts, 02139, USA

The MIT satellite team is currently constructing the Cathode/Anode Satellite Technology for Orbital Repositioning (CASTOR) satellite as part of the 6th University Nanosatellite Program (UNP-6) Flight Competition. The objective of the CASTOR satellite is to verify the on-orbit performance of the Diverging Cusped Field Thruster (DCFT) developed at MIT. The DCFT is an electrostatic thruster based on a cusped magnetic field configuration to confine ionizing electrons through a combination of processes, including magnetic mirroring. The DCFT is currently undergoing integration and performance testing for use on the CASTOR satellite. A power processing unit (PPU) has been developed to optimally operate the DCFT during the satellite mission. Preliminary testing with the PPU has been successful and has allowed for the next stage in development of the PPU.

Nomenclature

T = thrust
m_o = total wet mass
t = time
a = vehicle acceleration
P_a = anode power
η_t = anode thrust efficiency
c = exhaust velocity
I_{sp} = specific impulse
g = acceleration due to gravity
ΔV = velocity change

*Graduate Student, Department of Aeronautics and Astronautics, rmdaspit@mit.edu.
†Graduate Student, Department of Aeronautics and Astronautics, hancj@mit.edu.
‡Professor, Department of Aeronautics and Astronautics, plozano@mit.edu.
§Professor, Department of Aeronautics and Astronautics, millerd@mit.edu.

I. Introduction

Low power electric propulsion has become a viable option for satellite missions focused on station keeping and orbital repositioning where large delta V is required but low thrust is acceptable. Furthermore, this kind of propulsion would increase flexibility in the development of small satellites (< 100 kg) by enabling their maneuverability at reduced propellant mass fractions in comparison to chemical-based engines. Hall-effect thrusters belong to a type of electric thrusters that are useful for these missions by providing a specific impulse ranging from 1000-2000 seconds and thrust efficiency close to 50%.[1] Hall-effect thrusters accelerate ions through a quasi-neutral plasma and therefore are not space charge limited and can achieve high thrust densities.[2] In addition, they require relatively simple power processing units (PPU) when compared against other types of electric propulsion. Despite its advantages Hall thrusters have not received much attention in the United Stated until recent decades due to lower propulsive efficiency than ion engines. The first flight of a US-built Hall thruster (BHT-200) was onboard the AFRL TacSat 2 launched in 2006.[3] Improvements to Hall thruster performance have been attempted with altered magnetic configurations. In a radical modification, cusped fields have been proposed to boost engine performance. These types of thrusters have been developed by THALES Electron Devices, Princeton University, and MIT. The THALES High Efficiency Plasma Emitter (HEMP) was the first thruster to use the concept of cusped fields to provide both radial field regions, to initiate Hall currents, and wall protection through near parallel fields away from the cusps.[4,5] The Princeton Cylindrical Hall Thruster (CHT) employs similar electron trapping with cusps along the walls but also has a central cusp to produce an axial force on electrons.[6−8] The MIT DCFT has taken aspects from both designs. With its cusped magnetic field configuration, the DCFT belongs to these new kinds of electric thrusters and is expected to have longer a lifetime and improved efficiency by providing greater control over electron flux towards the anode and better overall trapping due to the different processes acting in this direction, e.g., magnetic mirroring, electrostatic sheaths, cross diffusion and regular cross-field drifts.[2,9−11] CASTOR is a 50 kg satellite that will use the DCFT as its main propulsion unit. The CASTOR satellite will provide a platform for the DCFT to obtain flight experience and demonstrate its functionality with a power system built around the DCFT.

II. University Nanosatellite Program Background

The University Nanosatellite Program is run jointly by the Air Force Research Laboratory's Space Vehicles Directorate (AFRL/RV), the Air Force Office of Scientific Research (AFOSR), and the American Institute of Aeronautics and Astronautics (AIAA).[12] The program is intended to educate current students through a national satellite design and construction competition and to enable the research, development, integration and flight testing of small satellites (< 50 kg). The University Nanosatellite Program consists of a selection phase and testing phase. The selection phase is a two year process where universities design and build a satellite and demonstrate progress at several design reviews. Satellites must be complete by the final review, the Flight Competition Review (FCR), where one satellite is selected for flight integration and progresses to the testing phase. In the test phase, the satellite is integrated with a separation system and is evaluated through several environmental tests leading to a potential launch opportunity.[12]

The FCR for UNP-5 occurred in January 2009. UNP-6 began shortly thereafter and completed the Preliminary Design Review this August. The winner of UNP-3 is currently planned for launch in December of 2009,[13] and the winner of UNP-4 began environmental testing in March 2008.[12] UNP-2 was concurrent with UNP-1 with a total of nine universities participating. Three produced flight qualified satellites, and two of those three were launched in December 2004.[12] A glitch in the launch vehicle released the satellites in a lower orbit than planned shortening the lifetime of the satellites such that no scientific information was obtained. Propulsion systems on university level satellites have been used for space situation awareness or atmospheric drag make up. To date, no satellite selected by UNP has attempted a high delta V propulsive maneuver.

III. MIT Satellite Program

The CASTOR satellite is being designed as part of UNP-6. The mission objectives of the CASTOR satellite are to operate the DCFT for 1500 hours and to measure the performance and characterize the degradation of the DCFT interior due to electron and ion impingement throughout the mission lifetime.[14]

The CASTOR satellite would be the first satellite at the university level to perform a high delta V maneuver. Given the program complexity, the mission would be considered a success, at the very minimum, if the DCFT can be shown to provide a measurable change in velocity.

The CASTOR satellite team is divided into five subteams Power/Propulsion, Orbits/Operations, Structures/Thermal, Attitude Determination and Control/Guidance Navigation and Control, and Avionics/Communications all overseen by a Systems/Management team. The structure of the CASTOR satellite is centered on the Xenon propellant tank for the DCFT and has 4 aluminum fins for mounting hardware and radiation plates. An on-board computer will control all electronic components of CASTOR. Two semi omnidirectional antennae will provide communication with the HETE ground station. The HETE ground station was built for communication with the High Energy Transient Explorer satellite and is operated by MIT. The antennae will be able to transmit data collected from the satellite to Earth and to receive updated commands or software from the HETE ground station if necessary. Positioning will be determined using a GPS tracker while gimballing of the DCFT and a reaction wheel will control the attitude. Nitrogen gas thrusters will be used to de-saturate the reaction wheel and will have a total delta V of 2 m/s. The power system uses deployable, sun-tracking solar panels and a rechargeable battery pack to provide 275 Watts to CASTOR which is regulated and distributed by the Electrical Power System (EPS). The EPS is composed of the PPU and the Power Distribution Unit (PDU). The PPU regulates the power for the DCFT while the PDU regulates the power for all other subsystems. The DCFT will be the primary propulsion unit on the CASTOR satellite. The DCFT is expected to operate for over 1500 hours performing a 1000 m/s velocity change. The CASTOR design is shown in Figure 1.

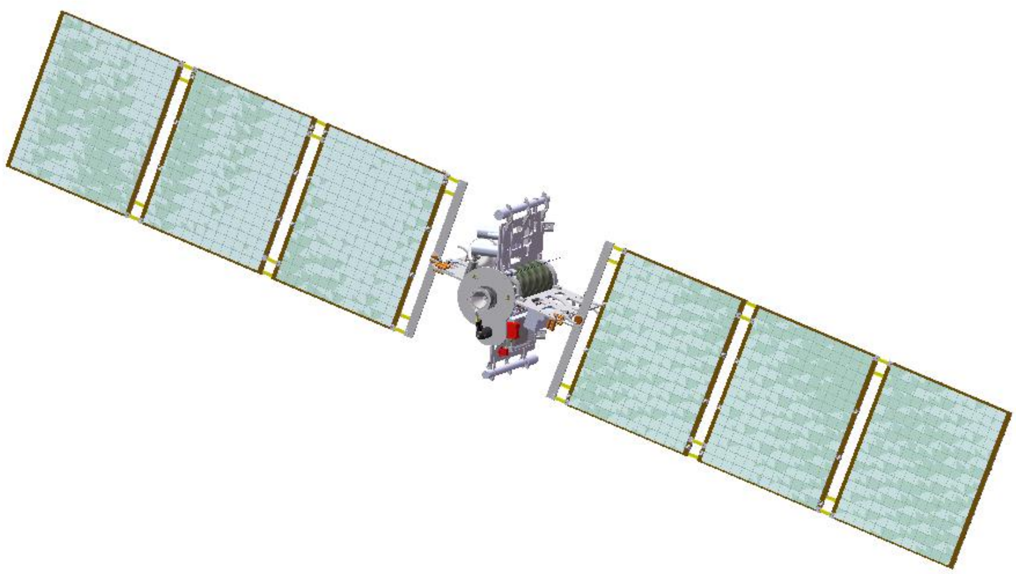

Figure 1. Solidworks model of the CASTOR satellite.

The CASTOR satellite team participated in the PDR of UNP-6 in August 2009 with many components having already been prototyped and tested. Some major successes were the demonstration of solar panel deployment on the Zero-G flight and the successful vibration testing of the CASTOR mass mockup shown in Figure 2 at Lincoln Labs. A full prototype will be built this coming December in preparation for the UNP Critical Design Review in January 2010.

IV. The Propulsion System

The CASTOR satellite propulsion system combines the DCFT, a barium oxide impregnated tungsten (BaO - W) hollow cathode, a Xenon propellant feed system, and a power processing unit to operate and produce thrust.

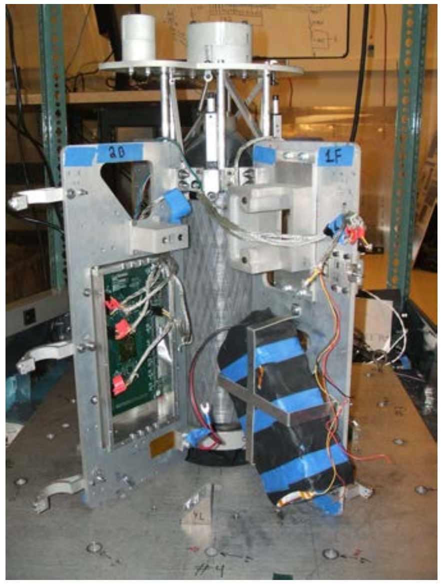

Figure 2. Mass mockup of the CASTOR satellite used for vibration testing.

A. Diverging Cusped Field Thruster

The DCFT is schematically illustrated in Figure 3. It is an electrostatic thruster with a modified magnetic configuration that uses a cusped magnetic field.[2,15,16] It uses three Samarium Cobalt magnets arranged such that repelling poles of the magnets are adjacent to one another creating two cusps and a magnetic gradient approaching the anode. The magnetic gradients confine electron movement in the conical section and prevent losses to the walls. The basic process for producing thrust is based on the ionization of Xenon atoms in the conical chamber, due to collisions with electrons, and the acceleration of those ions away from the anode due to the electric field created from the potential difference between the anode and cathode. Thrust is then conveyed to the body of the DCFT by the magnetic forces between the magnets and the captured electrons. The DCFT shows promise as a high delta V mission thruster for small satellites due to preliminary performance showing high efficiency at reduced power levels.[2,15] The DCFT is currently not optimized in regards to its size, magnetic strength, and cathode position as a function of power, yet it showed performance levels that are competitive with Hall devices.[2]

B. Busek BaO-W Hollow Cathode

The cathode used with the DCFT is the Busek BaO-W hollow cathode. The cathode consists of a heater for cathode conditioning at the beginning of the mission and a keeper to maintain an electron flow from the cathode at a low power. The conditioning phase at the beginning of the mission prevents cathode damage or contamination by heating the cathode in a slow and precise manner by controlling the current. A current of 2.0 A must be maintained to the heater for 90 minutes followed by 4.0 A for another 90 minutes and then 6.0 A for 30 minutes while at least 1 standard cubic centimeters per minute (sccm) of Xenon is provided to the cathode starting at least 30 minutes before conditioning begins and continuing while the cathode is operating.[17] The current can then be increased to 6.5 A for 10 minutes followed by the ignition of the keeper. Once the keeper is operating, the power to the heater can be decreased and then shut off. The keeper will maintain the internal heat of the cathode to operate at a lower power than the heater. The current to the keeper must be maintained at 0.5 A to prevent the keeper from not being able to sustain cathode operation or over heating. The heating process creates thermionic emission of Barium oxide within the cathode. The flow of Xenon atoms, Xenon ions, and electrons maintains a quasi-neutral plasma within the cathode for operation.[2]

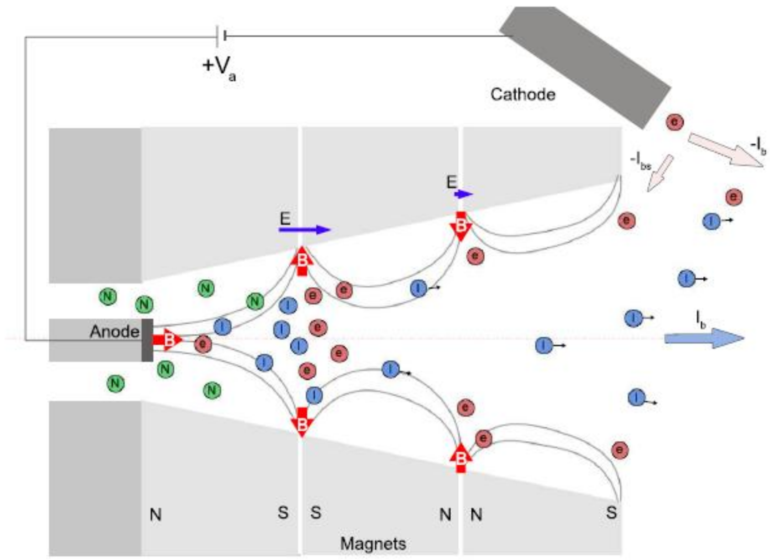

Figure 3. Schematic diagram of the DCFT basic operating principles.[2]

C. Xenon Propellant Feed System

A propellant feed system shown in Figure 4 was designed as part of the CASTOR satellite to ensure the proper amount of Xenon is supplied to the DCFT and cathode system. The feed system consists of a high pressure side (4500 psi) and a low pressure side (15 psi). The propellant tank holds 5 kg of pressurized Xenon in order to achieve at least 1500 hours of nominal operation. The high pressure side also consists of a manual value for tank filling purposes and a pressure relief valve that will release Xenon to depressurize the system and prevent it from bursting should it become over pressurized. A pressure regulator reduces the pressure of the Xenon for use in the DCFT. Two solenoid valves are placed such that flow can be shut off to either the anode or both the anode and cathode simultaneously at predetermined times during the mission. One flow regulator is placed before the cathode and one before the anode in order to ensure adequate flow is provided to the anode and cathode. Flow regulators will be able to measure and control xenon flow to 0-10 sccm.

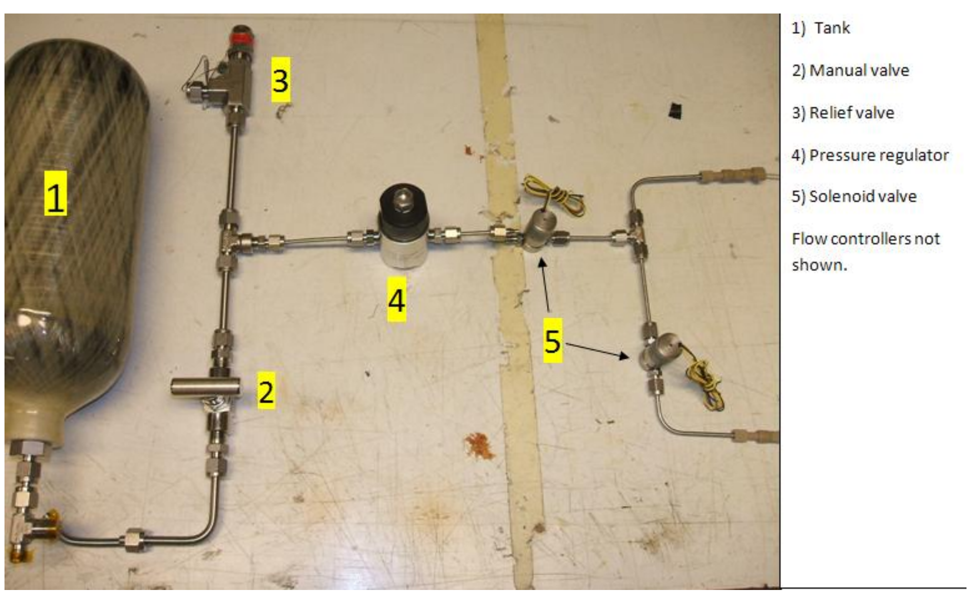

Figure 4. Propellant feed system for the DCFT.

D. Power Processing Unit

The PPU shown in Figure 5 controls the power provided to the DCFT. The solar cells will produce 275 W for the CASTOR satellite during sunlight and will output a constant 24 V. A maximum power point tracker (MPPT) will be used to charge the batteries and provide the rest of the power to the satellite through the PDU and PPU. During eclipse, the MPPT will use the batteries to power essential components of the satellite. The PPU will regulate the power for the thruster system, namely the cathode (heater and keeper) and anode, while the PDU will regulate power to all other components of the spacecraft. The PPU provides power for three different components of the thruster, each with its specific power requirements. The heater converter will regulate the voltage in progressive steps from 0-12 V, to provide a gentle increase of the temperature profile during cathode conditioning. Cathode conditioning is generally performed with current control, but voltage control was chosen due to ease of implementation and weight savings. In preliminary tests, voltage control was found to be sufficient in recreating the cathode conditioning profile. After conditioning is complete, the keeper converter will provide 0.5 A constant current to the keeper as the heater shuts off. The anode converter will supply 200 V to the anode for DCFT operation during sunlight once the keeper has been ignited. During eclipse, the anode converter will be shut off and the keeper converter will remain on in order to quickly resume DCFT operation when in sunlight again. The PPU on/off and trim control will be powered by 5 V, provided by the PDU and controlled by an onboard computer.

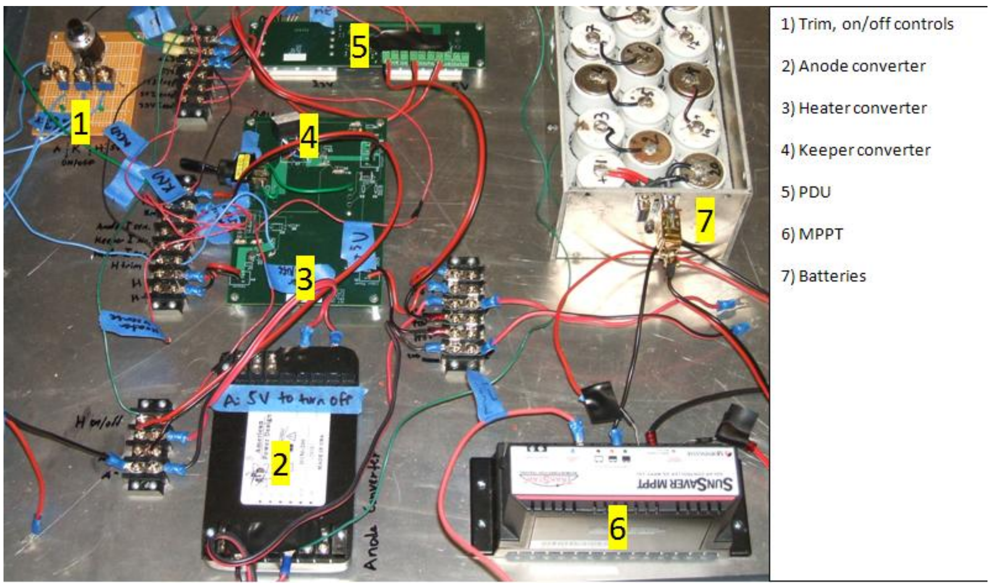

Figure 5. Current configuration of the PPU. Used with testing described in this paper.

V. DCFT Application

The use of the DCFT on the CASTOR satellite will provide invaluable flight experience to the DCFT development program by providing information about the operation of the DCFT in orbit. The options for nanosatellites (50-100 kg) to have propulsion systems for large delta V missions (> 1 km/s) are limited, so the success of the DCFT onboard CASTOR will provide a functional propulsion system (thruster, PPU, and propellant feed system) for use on nanosatellites. The DCFT is also expected to have a longer lifetime and less energy losses than similar thrusters due to its cusped magnetic configuration that limits electron and ion impingement on the boron nitride cone reducing its degradation.[2,9–11] Creating a lightweight, high specific impulse, high efficiency propulsion system (1 kg PPU, 2 kg thruster, 5 kg propellant system, 1300 sec, 45% efficiency) for use on nanosatellites will open up new missions for these satellites that cannot accommodate the large propellant mass fraction of chemical thrusters or the complex power systems of other electric thrusters. We calculated the expected flight performance parameters for the DCFT with Eqns. 1, 2, 3, and 4 using data from previous tests.[2]

$$\Delta V = at \tag{1}$$

$$T = \frac{2P_a\eta_t}{c} \tag{2}$$

$$T = m_o a \tag{3}$$

$$I_{sp} = \frac{c}{g} \tag{4}$$

VI. CASTOR Mission

The CASTOR satellite is designed for a low Earth orbit of about 500 km from the Earth's surface with an orbital period of 90 minutes. The entire mission will last approximately 250 days will a total DCFT firing time of about 1500 hours. The mission will consist of a deployment stage, a commissioning stage, a normal operation stage, and a decommissioning stage. The batteries will be charged and all systems except the propulsion system will be turned on during the deployment stage. Cathode conditioning will occur during the commissioning stage. The DCFT will fire only during the sunlight portions of each orbit for about 45 minutes during normal operations. Based on DCFT performance during previous testing, the DCFT will provide approximately 10 mN of thrust accelerating the CASTOR satellite at 0.0002 m/s^2. Several sensors and a camera will be used to monitor the DCFT's performance and degradation while in orbit. Each orbit with the DCFT thrusting will change the satellite's velocity by 0.54 m/s. After 125 days of normal operation, the DCFT will achieve a delta V of over 1000 m/s. The satellite will increase and decrease its orbit during the normal operation stage. The decommissioning stage will be an uncontrolled atmospheric re-entry.

VII. DCFT Modifications for UNP

The initial design of the DCFT is discussed thoroughly in the prior literature.[2,15–16] The current design of the DCFT is a smaller and lighter version, specifically for use on the CASTOR satellite. The new DCFT variant was designed and constructed by the MIT satellite team with the intent of reducing the size and mass to meet program requirements while retaining the operational characteristics of the initial incarnation. To this end the non-magnetic stainless steel outer casing was replaced with a thinner aluminum shell and the thickness of the 1018 steel core was reduced. The base core reduction was undertaken with minimal impact on the magnetic field topology as demonstrated in Figure 6.[18]

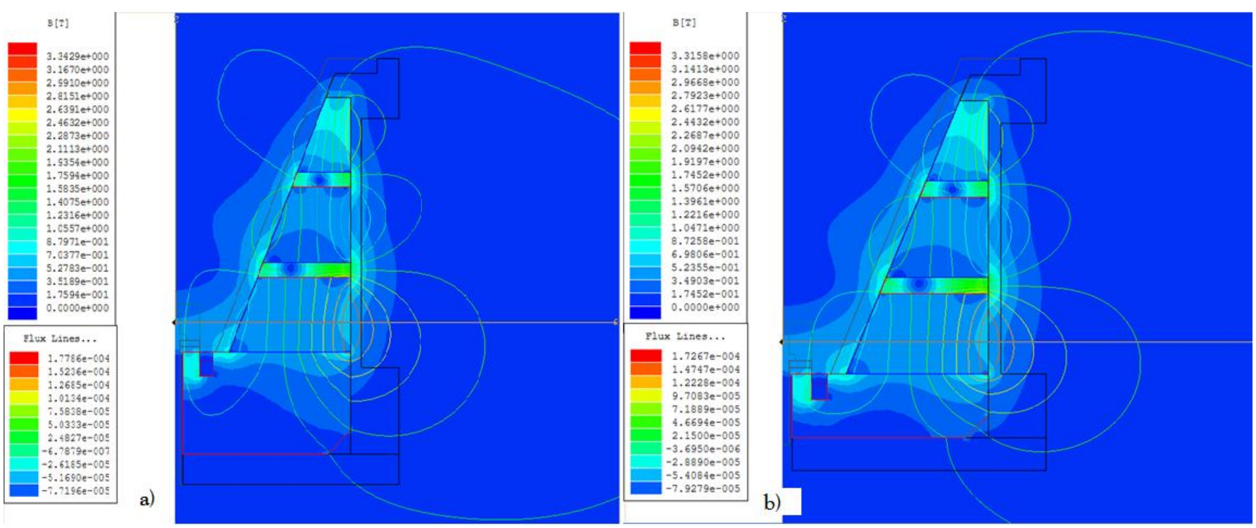

Figure 6. Magnetic topology on the r-z plane for the DCFT from (a) Previous Work and (b) the Current Study.[18] Found using Ansoft Maxwell SV software.

Alterations were made to the anode design based on lessons learned from prior constructs. Electrical connections are made at the rear of the thruster to a 316 stainless steel anode stem, which is threaded on the opposite end to allow the use of various materials for the current collecting anode cap. Currently, only graphite caps are in use for the anode due to their low sputtering yield and ease of machining. The upstream end of the anode cap is kept 2 mm from the base core by HP grade Boron Nitride spacers.

The attachment from the Xenon propellant feed system to the DCFT and components within the DCFT were altered to provide a more reliable flow of Xenon into the cone of the DCFT. Arcing was occasionally observed in the older DCFT version which was attributed, potentially, to Xenon becoming trapped under the cone and anode. From the feed system, xenon enters into the back of the core and then exits through a porous steel ring at the front of the core to enter the cone chamber. In the first version of the DCFT, the ring was partially covered by the anode and the bottom edge of the cone. The inner and outer radii of the porous steel piece were both reduced in the second version so that it was no longer partially covered by the anode or cone preventing any possible trapping of Xenon near there. Arcing was also attributed to a potential leak in the DCFT-propellant feed system connection. The tubing that connected to the core was originally threaded on the outside, and the core was tapped so that the tube screwed into place. This may have not provided a satisfactory seal, so the tubing was vacuum welded to the core to prevent any potential leaks.

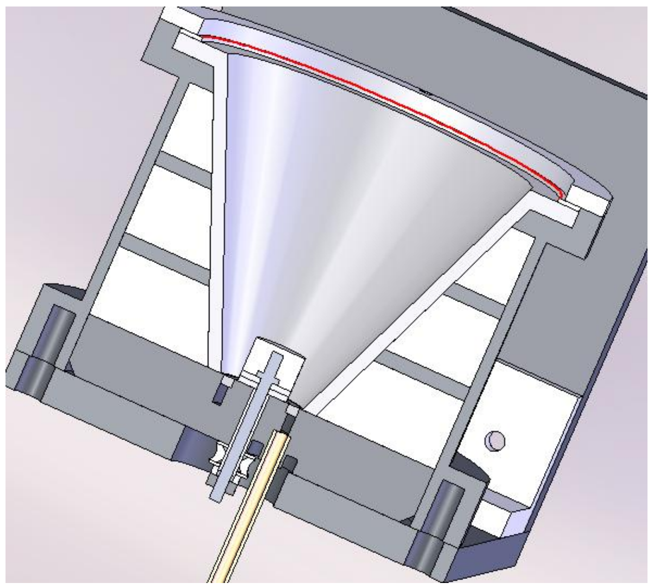

Figure 7. Solidworks model of new DCFT design.

VIII. Experimental Procedures

A. Facility

All DCFT testing was performed in the MIT Space Propulsion Laboratory ASTROVAC vacuum chamber. The vacuum chamber has a 1.5 m diameter by a 1.6 m depth and is equipped with two CTI cryopumps capable of pumping roughly 7500 L/s of Xenon. Two Omega mass flow controllers are connected to the chamber to provide flow control and measurement to the cathode and anode from 0-10 sccm. The facility also has two 1.0 kW Sorensen DC programmable power supplies to provide power to the keeper and anode, and a BK Precision DC regulated power supply to provide power to the heater. All of the SPL power sources could be either voltage or current controlled. The DCFT body was left floating electrically while the anode and cathode potentials were applied with respect to a common ground in the chamber. The testing described in this paper was the PPU-DCFT integration test to verify the cathode and DCFT could operate from conditioning to thrusting with power regulation from the PPU.

B. Operational Procedures

The first test performed used the SPL power sources for conditioning to record the conditioning operating points (voltage, current, and time) with a current controlled power supply. This allowed us to determine when to vary the voltage of the heater converter to maintain the correct current for conditioning procedure. Voltage and current were recorded every 5-10 minutes from the display on the power source. We were unable to ignite the heater with 2.0 Amps, so 2.5 Amps were used. The voltages for the set currents are shown as a function of time in Figure 8. The internal resistance and the power drawn were calculated from the data recorded.

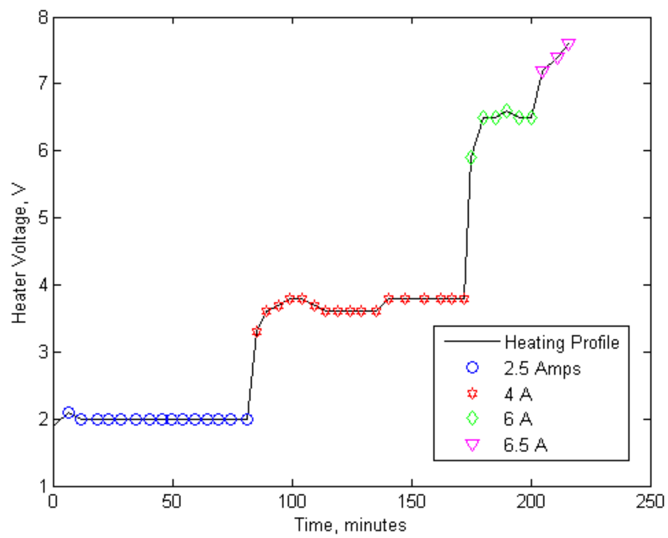

Figure 8. Heater voltage for given currents duing conditioning.

The power required to condition the cathode graphed in Figure 9 will affect the power available to the rest of the CASTOR satellite. This data will be used to determine how to allocate the remaining power to the other systems on the CASTOR satellite during cathode conditioning.

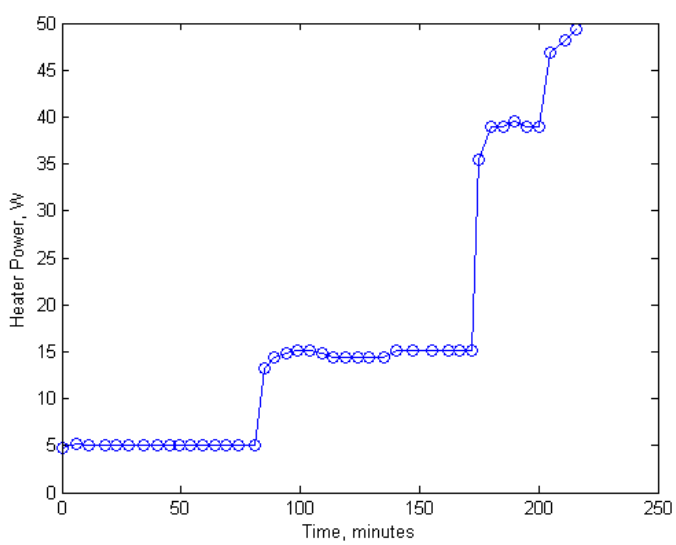

Figure 9. Heater power during conditioning.

Ignition of the keeper occured after conditioning was completed. The current supplied to the heater was then decreased. Power was then supplied to the anode and a blue plume was observed due to excited Xenon ions exiting from the cone. A 200 V operating point for the anode was used as it corresponds to the voltage output of the anode converter. The power to the heater was shut off 10 minutes after the anode was turned on. The keeper maintained the heat within the cathode after the heater was shut off. After observing the DCFT was operating stably as in Figure 10, the anode and keeper were shut off and the cathode was allowed to cool for 30 minutes.

Figure 10. DCFT during operation in the ASTROVAC.

The DCFT and cathode were then disconnected from the SPL power sources and connected to the PPU. Power was provided by an HP 1200 W power supply which was connected directly to the PPU. The output voltage was set at 24 V to simulate solar panel output with a maximum power of 1200 W. A secondary power supply was used to provide power to the on/off switches to the PPU converters and the manual trim dial to the heater converter. A dial was used to trim the output voltage of the heater converter. Multimeters were placed to record the current through the main power supply and the anode, heater, and keeper converters. A fifth multimeter was used to measure the voltage across the three converters. Measurements were again taken in approximately 5 minute intervals. Although the onboard computer will regulate the trim on the CASTOR satellite, a manual dial and switches were used for the tests described in this paper.

IX. Results and Discussion

Because the cathode was still warm and all possible contaminants had already been purged from the previous conditioning, a shortened conditioning could be used as a careful heating profile was no longer needed. A shortened conditioning is planned because of the nearly constant values of heater voltage for different current. Once a stable current was achieved at each step in the conditioning process, the cathode was heated to the next current step. The heater ignited at 2.3 V with a current of 2.06 A. The voltage and current both slowly increased until they became stable near 2.34 V and 2.29 A. The voltage across the heater was then increased to 4.26 V to increase the current to 3.98 A. The voltage was increased a few more times until the current remained stable near 4.0 A. When the voltage was increased for the next current step, the current maxed out at 4.54 A with a voltage of 5.54 V. It was soon discovered that the heater converter's maximum power output was trimmed when the voltage output was trimmed. The converter has a 50 W maximum power output for the maximum voltage output of 12 V. At 5.54 V, the maximum power output is approximately 23 W so the current was unable to increase above 4.54 A. The full set of data for voltage, current, and power as functions of time as well as the converter power limit as a function of voltage are included in Figure 11.

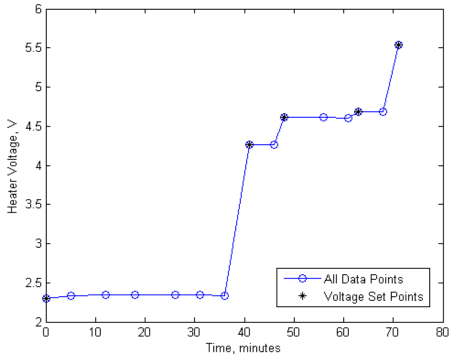

(a) Heater voltage as a function of time. Manual increases to the voltage using the trim are indicated with a star.

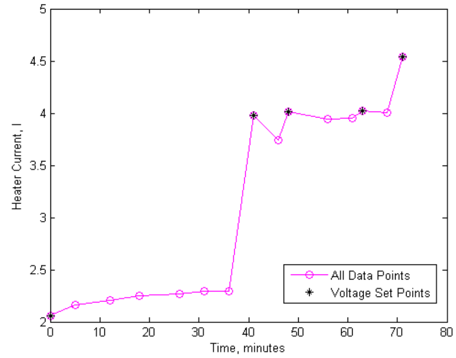

(b) Heater current as a function of time. Manual increases to the voltage using the trim are indicated with a star.

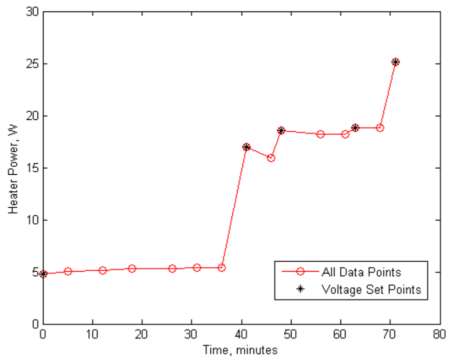

(c) Heater power as a function of time. Manual increases to the voltage using the trim are indicated with a star.

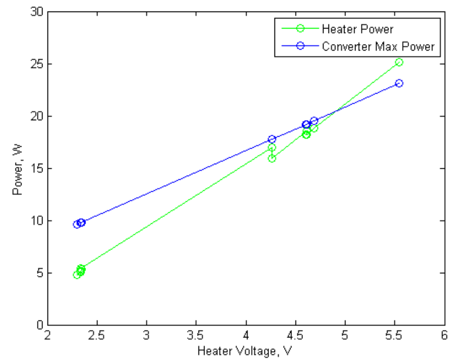

(d) This graph shows the heater's power consumption and the converter's power limit as a function of heater voltage. Near 5 V the heater attempts to draw more power than the converter can supply.

Figure 11. Cathode conditioning with PPU.

The voltage during the conditioning using the PPU was noticeably higher for given currents as shown in Figure 12. This was attributed to not allowing the cathode enough time to cool down. The cathode internal resistance increases as it is heated so inadequate cooling time caused the resistance to remain high. It is important for the temperature to follow a specific heating profile during conditioning on board CASTOR so future tests will have time alloted for the cathode to adequtely cool down.

Once the maximum power problem with the heater converted was diagnosed, the heater was disconnected from the PPU and reconnected to the SPL power source to complete conditioning. The rest of the PPU remained connected to the DCFT and cathode. The keeper converter was switched on and immediately ignited the keeper. The current through the keeper current remained at 0.5 A for the entire test. The voltage was 10.53 V initially and increased as the heater power was decreased. The anode converter was turned on while the heater voltage was being turned down. The blue plume due to ionization of Xenon was again observed coming from the cone. The anode voltage and current were measured to be 185.3 V and 0.69 A, respectively. The heater converter was switched off and the keeper began to draw more power. The keeper voltage increased to 23.88 V while the current remained at 0.5 A. After a few seconds at 23.88 V, the keeper unexpectedly shut off causing the cathode and DCFT to stop operating. The keeper converter maximum output voltage is 24 V which coincides with the expected keeper voltage of 24 V while the heater is off. Likely, the keeper voltage was trying to increase slightly above 24 V and was unable to so the keeper was unable to maintain ionization within the cathode and shut off. Graphs of the keeper operation are shown in Figure 13.

To test this hypothesis, the keeper was then disconnected from the PPU and reconnected to the SPL power source. The heater was turned on again and was set to output 6.5 A to reheat the cathode for 5

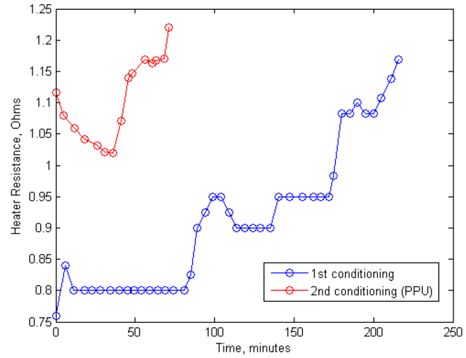

Figure 12. Cathode resistance during conditioning.

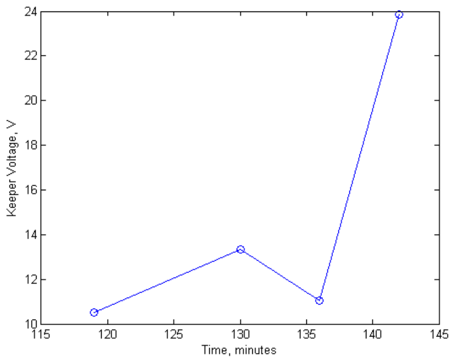

(a) Keeper voltage as a function of time. The keeper shut off after reaching the maximun shown on the graph.

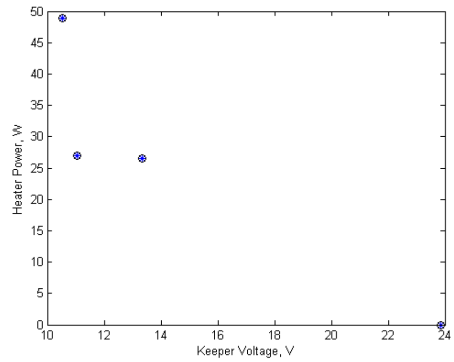

(b) Keeper voltage vs. heater power. As the heater power was decreased, the keeper voltage steadily increased to the converter's limit.

Figure 13. Keeper operation.

minutes if any cooling had occurred. The keeper power source voltage maximum was set at 30 V and the keeper was re-ignited at 0.5 A. The current to the heater was slowly decreased to 0 A. The keeper voltage began to rise and settled at 24-25 V, close to the PPU limit, thus verifying that the keeper converter was limiting the voltage.

X. Conclusion and Future Work

The first integration test of the DCFT and PPU is complete. The DCFT-PPU integration test at MIT proved the functionality of the DCFT with the PPU albeit a few problems with the converters. All of the converters were able to power their respective DCFT components and the problems encountered can be easily corrected with the proper redesign of the PPU allowing this test to be considered successful.

The redesign of the PPU has already been complete, and we are awaiting the arrival of the new components. A new heater converter was selected that has a 100 W maximum output at a 12 V maximum voltage output. The power output is still decreased when the voltage output is trimmed but is now well above the required heater power. A new keeper converter was selected that has a maximum voltage output of 36 V. The flight computer has also recently been completed so that the next test will be completely automated, and we will not have to manually control the converters.

An integration test with the propellant feed system is planned for the future. The propellant feed system is complete and will be going through its own operational testing before integration testing is attempted. The feed system will be tested with inexpensive argon to ensure all components operate properly for use in the DCFT.

Finally, a thrust balance shown in Figure 14 has been designed and is currently being constructed in order to measure thrust and efficiency of the DCFT. The balance is a vertical see-saw that will rotate as the DCFT produces thrust. The balance uses a voice coil, LVDT, and flexures to dampen and measure the amount of thrust created. The efficiency and specific impulse can then be calculated using the mass flow of Xenon, and the power provided to the anode. The information gained from testing the DCFT with the thrust balance will be used to optimize the voltage output of the anode converter. The current output was selected based on previous testing that measured the thrust for various anode voltages using the first DCFT design.[2]

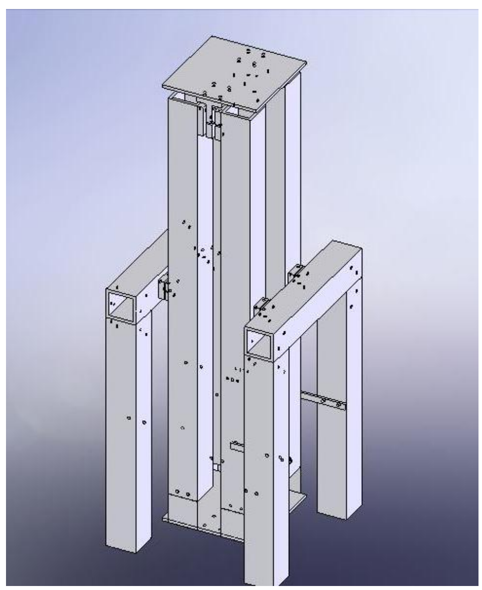

Figure 14. Solidworks model of thrust balance.

Optimization of the magnetic field, cathode position relative to the DCFT, and size of the DCFT as a function of power is also planned in the future after integration testing is complete.

Acknowledgments

The authors would like to thank members of the MIT Satellite Team for their work on the PPU. The authors would especially like to thank Dan Courtney for all of his assistance with the DCFT and Busek for loaning us a cathode to complete testing while our cathode was inoperable.

References

[1]Martinez-Sanchez, M. and Pollard, J. E., "Spacecraft Electric Propulsion - An Overview," *Journal of Propulsion and Power*, Vol. 14, No. 5, 1998, pp. 688-699.

[2]Courtney, D., "Development and Characterization of a Diverging Cusped Field Thruster and a Lanthanum Hexaboride Hollow Cathode," Masters Thesis, Massachusetts Institute of Technology, 2008.

[3]Busek Co., www.busek.com.

[4]Kornfeld, G., Koch, N., and Coustou, G., "First Test Results of the HEMP Thruster Concept," *28th International Electric Propulsion Conference*, Toulouse, France, March 2003, also IEPC-03-134.

[5]Kornfeld, G., "Plasma Accelerator Arrangement," United States Patent 6,523,338 B1, 2003.

[6]Raitses, Y. and Fisch, N. J., "Parametric Investigations of a Nonconventional Hall Thruster," *Physics of Plasmas*, Vol. 8, No. 5, 2001.

[7]Smirnov, A., Raitses, Y., and Fisch, N. J., "Experimental and Theoretical Studies of Cylindrical Hall Thrusters," *Physics of Plasmas*, Vol. 14, No. 057106, 2007.

[8]Raitses, Y. and Fisch, N. J., "Cylindrical Geometry Hall Thruster," United States Patent 6,448,721 B2, 2002.

[9]Sovey, J.S. "Improved Ion Containment Using a Ring-Cusp Ion Thruster," *Journal of Spacecraft and Rockets*, 1984.

[10]Smirnov, A., Raitses, Y., Fisch, N.J., "Electron cross-field transport in a low power Cylindrical Hall Thruster," *Physics of Plasmas*, 2004.

[11]Kornfeld, G., Koch, N., Harmann, H., "Physics and Evolution of HEMP-Thrusters," *30th International Electric Propulsion Conference*, Florence, Italy, September 2007, also IEPC-2007-108.

[12]University Nanosatellite Program, www.vs.afrl.af.mil/UNP.

[13]University of Texas Nanosatellite Program, "FASTRAC," fastrac.ae.utexas.edu.

[14]MIT Satellite Team, "CASTOR," satellite.mit.edu.

[15]Courtney, D., Martinez-Sanchez, M., "Diverging Cusped-Field Hall Thruster (DCHT)," *30th International Electric Propulsion Conference*, Florence, Italy, September 2007, also IEPC-2007-037.

[16]Courtney, D., Lozano, P., Martinez-Sanchez, M., "Continued Investigation of Diverging Cusped Field Thruster," *44th AIAA/ASME/SAE/ASEE Joint Propulsion Conference*, Hartford, Connecticut, July 2008, also AIAA-2008-4631-556.

[17]Busek Hollow Cathode BHC-1500 Operating and Maintenance Manual, July 2008.

[18]Matlock, T., Daspit, R., Batishchev, O., Lozano, P., Martinez-Sanchez, M., "Spectroscopic and Electrostatic Investigation of the Diverging Cusped-Field Thruster," *45th AIAA/ASME/SAE/ASEE Joint Propulsion Conference*, Denver, Colorado, August 2009.